Dalton Transactions

PAPER

View Article Online
View Journal | View Issue

Cite this: *Dalton Trans.*, 2014, **43**, 15812

Synthesis and crystal structure of a series of incommensurately modulated composite oxohalide compounds†

Iwan Zimmermann,[a] Alexis Corgnet,[a] Mats Johnsson*[a] and Sven Lidin[b]

Received 9th July 2014,
Accepted 26th August 2014

DOI: 10.1039/c4dt02084g

www.rsc.org/dalton

Transparent, needle-like single crystals of the isostructural compounds $[Sb_4O_{7+3\delta}X_4][Zn_3]_{1+\delta}$ (X = Cl, Br, I) $\delta \approx 0.2$ were obtained from chemical reactions in evacuated and sealed silica tubes. First, the average structure was solved in $P2_1/n$ but the model refined poorly and a lowering of the symmetry to the 3 + 1 dimensional space group $P2_1(\alpha 0\gamma)0$ gave a significantly better fit to the data. This model used second order positional modulations for all the atoms. Whereas Sb, Cl (Br, I) and most O positions were well behaved, there was a mismatch with Zn that was better described in a sub-cell, thus yielding a composite structure. The composite nature of the structure leads to a charge imbalance that is compensated by oxygen vacancies.

Introduction

A rich structural variety exists among oxides and oxohalides containing antimony because of the flexibility of the coordination of Sb^{3+}. The stereochemically active lone-pair on Sb^{3+} causes an asymmetric coordination, and the most common coordination polyhedra are $[SbO_3]$ trigonal pyramids and $[SbO_4]$ see-saws.

For ternary Sb–O–X (X = Cl, Br, I) compounds, there is a tendency for the halide ion to take the role of a counter ion rather than forming covalent bonds with antimony. For quaternary compounds also containing a late transition metal, it is most common that antimony only coordinates with oxygen and the transition metal bond to both oxygen and halide ions. This results in the formation of non-bonding volumes in the crystal structure between chalcogen/chalcophile and halogen/halophile parts, where the terminal halogens and lonepairs become next neighbors. The most reasonable explanation for this behavior is that they are excluded from the bonding subvolume of the structure rather than being attracted to each other. The flexibility in the coordination around Sb^{3+} and its preference to bond only to oxygen led to several types of antimony oxide entities, *e.g.* small cages resembling cubic Sb_2O_3 in $CuSb_2O_3Br$,[1] bigger cages resembling zeolite β-cages in $Cu_{20}Sb_{35}O_{44}Cl_{37}$,[2] layers in $CuSbTeO_3Cl_2$[3] and tubes in $Sb_8O_{11}X_2$.[4–6] In this work, we present the isostructural compounds $[Sb_4O_{7+3\delta}X_4][Zn_3]_{1+\delta}$ (X = Cl, Br, I), $\delta \approx 0.2$ with a rather simple columnar average structure that actually proved to be a composite structure, in which the Zn atoms are best described in a sub-cell. Composite structures are relatively rare and are mainly observed among intermetallic compounds and among sulfides and fluorides.[7] However, the latter are mostly layer misfit compounds, and there is also a good example of columnar misfit: the "alchemist's gold", $Hg_{2.86}AsF_6$.[8,9] Oxide-based, modulated composite structures have been found in several hexagonal perovskites and related materials such as *e.g.* $Sr_{1.2872}NiO_3$,[10] $Sr_{1+x}(Co_xMn_{1-x})O_3$,[11] $Ba_{1+x}[(Cu_xRh_{1-x})O_3]$[12] and $Sr_{1+x}(Cu_xMn_{1-x})O_3$.[13] To the best of our knowledge the present compounds are the first oxohalides to show a composite structure.

Experimental

Transparent, needle-like single crystals of the compounds $[Sb_4O_{7+3\delta}Cl_4][Zn_3]_{1+\delta}$, $[Sb_4O_{7+3\delta}Br_4][Zn_3]_{1+\delta}$ and $[Sb_4O_{7+3\delta}I_4][Zn_3]_{1+\delta}$, $\delta \approx 0.2$ were obtained from chemical reactions in evacuated and sealed silica tubes. ZnO (ABCR), $ZnCl_2$ (Sigma-Aldrich), $ZnBr_2$ (Sigma-Aldrich), ZnI_2 (ABCR) and Sb_2O_3 (Sigma-Aldrich) were used as starting materials. For the synthesis, a 1 : 1 : 1 mixture of ZnX_2 (X = Cl, Br, or I), ZnO_2 and Sb_2O_3 was subsequently heat treated at 550 °C for 60 h. Single

[a]*Department of Materials and Environmental Chemistry, Stockholm University, SE-106 91 Stockholm, Sweden. E-mail: mats.johnsson@mmk.su.se; Fax: +46-8-152187; Tel: +46-8-162169*
[b]*Department of Chemistry, Division of Polymer & Materials Chemistry, Lund University, Box 124, SE-221 00 Lund, Sweden*

† Electronic supplementary information (ESI) available: Further details on crystal structural investigations can be obtained from the Fachinformationszentrum Karlsruhe, Abt. PROKA, 76344 Eggenstein-Leopoldshafen, Germany (fax +49-7247-808-666; E-mail: crysdata@fiz-karlsruhe.de) on quoting the following depository numbers: CSD 427521 for $[Sb_4O_{7+3\delta}Cl_4][Zn_3]_{1+\delta}$, CSD 427522 for $[Sb_4O_{7+3\delta}Br_4][Zn_3]_{1+\delta}$, and CSD 427523 for $[Sb_4O_{7+3\delta}I_4][Zn_3]_{1+\delta}$.. See DOI: 10.1039/c4dt02084g

Table 1 Crystallographic information for $[Sb_4O_{7+3\delta}X_4][Zn_3]_{1+\delta}$ (X = Cl, Br, I), $\delta \approx 0.2$

Compound	$[Sb_4O_{7+3\delta}I_4][Zn_3]_{1+\delta}$	$[Sb_4O_{7+3\delta}Br_4][Zn_3]_{1+\delta}$	$[Sb_4O_{7+3\delta}Cl_4][Zn_3]_{1+\delta}$
Space group	$P2_1(\alpha 0 \gamma)0$	$P2_1(\alpha 0 \gamma)0$	$P2_1(\alpha 0 \gamma)0$
Symmetry operators	$x1, x2, x3, x4$ $-x1, x2 + 0.5, -x3, -x4$	$x1, x2, x3, x4$ $-x1, x2 + 0.5, -x3, -x4$	$x1, x2, x3, x4$ $-x1, x2 + 0.5, -x3, -x4$
a/Å	4.2710(8)	4.1307(13)	4.0634(6)
b/Å	18.508(3)	17.9042(2)	17.163(2)
c/Å	10.6741(14)	10.3021(10)	10.4699(13)
β/°	90.054(13)	90.331(6)	91.024(11)
q	$\begin{pmatrix} 0.2274(7) \\ 0 \\ 0.4236(15) \end{pmatrix}$	$\begin{pmatrix} 0.226(3) \\ 0 \\ 0.399(6) \end{pmatrix}$	$\begin{pmatrix} 0.2032(5) \\ 0 \\ 0.3602(12) \end{pmatrix}$
Crystal colour/habit	Colourless/needle	Colourless/needle	Colourless/needle
Crystal dimensions	0.32 × 0.04 × 0.03	0.21 × 0.03 × 0.02	0.20 × 0.04 × 0.02
No. of reflections all/$[I > 3\sigma(I)]$	16 749/4073	26 084/6011	22 220/3537
Goodness of fit S	1.51	2.02	1.39
R factors $[I > 3\sigma(I)]$	$R_1 = 0.0729$ (w$R_2 = 0.0711$)	$R_1 = 0.0982$ (w$R_2 = 0.1015$)	$R_1 = 0.0714$ (w$R_2 = 0.0690$)
Equivalents	$R_{int} = 0.0701$	$R_{int} = 0.1192$	$R_{int} = 0.1486$
Main reflections	$R = 0.0556$ (2355)	$R = 0.0808$ (3201)	$R = 0.0592$ (2302)
First-order satellites	$R = 0.1180$ (1610)	$R = 0.1297$ (2316)	$R = 0.1103$ (1003)
Second-order satellites	$R = 0.1751$ (108)	$R = 0.1920$ (494)	$R = 0.1580$ (232)
Residual e^- density (min/max)/Å^{-3}	4.23/−4.84	13.86/−9.56	9.13/−9.04

crystals were separated manually from unreacted starting material and crystals of the previously described compound $ZnSb_2O_4$[14] that was observed in minor amounts as by-product. Attempts to synthesize a corresponding oxofluoride phase starting with ZnF_2 as a fluorine source failed.

Single-crystal X-ray diffraction experiments were carried out on an Oxford Diffraction Xcalibur3 diffractometer equipped with a graphite monochromator. The data collection was at 293 K using MoKα radiation, $\lambda = 0.71073$ Å. Data reduction was performed with the software CrysAlis RED, which was also employed for the analytical absorption correction. The crystal structures were solved by charge flipping implemented in SUPERFLIP[15] and refined by full matrix least squares on F using the program JANA-2006;[16] the W matrix was calculated according to van Smaalen.[17,18]

The structural drawings are made with the program DIAMOND.[19] Powder patterns were collected on a Panalytical X'Pert PRO powder X-ray diffractometer in Bragg-Brentano geometry with Cu-K_α radiation. IR spectra were recorded on a Varian 670-IR FTIR spectrometer in the range 390–4000 cm^{-1} at ambient temperature. The spectrometer was equipped with an attenuated total reflection (ATR) detection device with a single reflection ATR diamond element. Thermogravimetric studies were performed in a Perkin-Elmer TGA7 unit in nitrogen with a heating rate of 5 °C min^{-1}.

Results

An inspection of reciprocal space images from compounds $[Sb_4O_{7+3\delta}X_4][Zn_3]_{1+\delta}$ (X = Cl, Br, I), $\delta \approx 0.2$ clearly show that the structures are incommensurately modulated with a $\boldsymbol{q}$ vector in the *ac*-plane of the fundamental monoclinic unit cell. The close-to-perfect orthorhombic pseudo-symmetry of the fundamental unit cell and the presence of two (orthorhombically) symmetry-equivalent $\boldsymbol{q}$-vectors clearly indicates that pseudo-merohedral twinning according to the orthorhombic-monoclinic symmetry lowering is expected. All the structures contain a set of strong substructure reflections and a set of weaker satellites that appear to be incommensurate with the substructure.

The crystallographic information of the three compounds is summarized in Table 1. The value of δ is given by the $\boldsymbol{q}$ vector component along a^*. The patterns further share the special feature that first-order satellites dominate for the 1*kl* reflections,

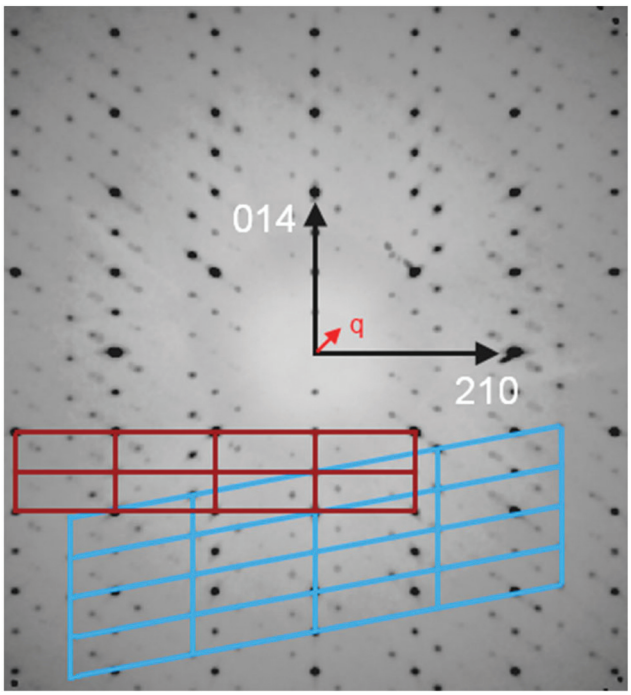

Fig. 1 Reconstructed reciprocal lattice section *hkl* integrated from k = 0 to k = 4 of the iodide compound. Note the relative intensity of first-order satellites for 1*kl* reflections and second-order satellites for 2*kl* reflections. Primary and secondary unit cells are indicated in red and blue, respectively.

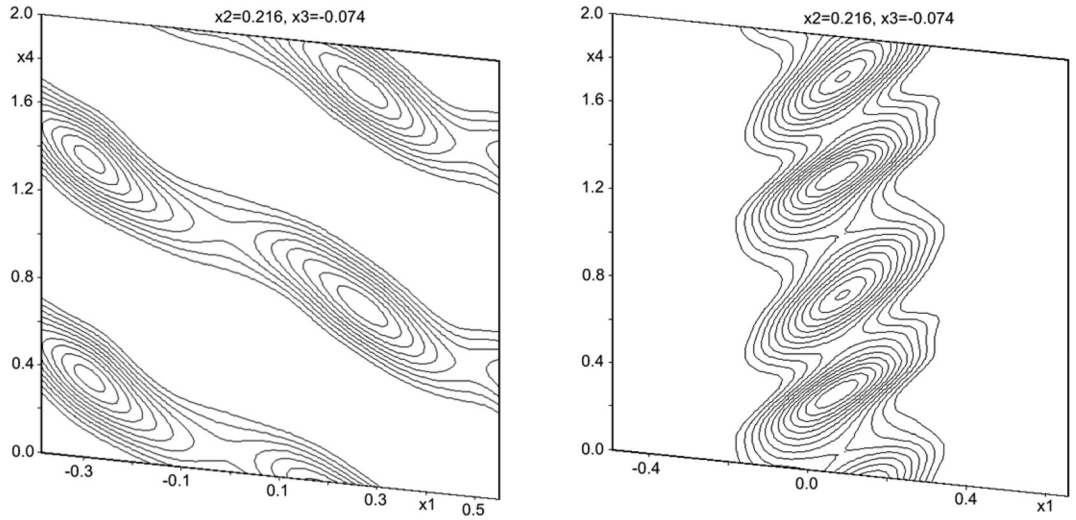

Fig. 2 Electron density map of Zn1 in the primary (left) and the secondary unit cells (right).

and the second-order satellites dominate for the $2kl$ reflections, as shown in Fig. 1. This is a strong indication for composite behavior.

Structural solutions using charge flipping in superspace (superflip) of the compounds was relatively straight-forward. A first structural solution was carried out in the centro-symmetric space group $P2_1/n$ but this solution refined rather poorly. Lowering the symmetry to Pn did little to improve the situation, whereas a model in the 3 + 1 dimensional space group $P2_1(\alpha 0\gamma)0$ provided a considerably better fit to the data. This model used second-order positional modulations for all the atoms. The automatic procedure produced excellent starting positions and modulations for Sb and halides, whereas the modulations for Zn turned out to be very large. Oxygen positions were only localized to some extent. The amplitude of the modulation of Zn positions was particularly large along the a direction, and while this could be modeled as a saw-tooth type positional modulation, it was clear that a composite structure model would be more suitable (see Fig. 2). After moving all the Zn positions to the secondary unit cell using the transformation matrix expressed as

$$W_2 = \begin{pmatrix} 1 & 0 & 0 & 1 \\ 0 & 1 & 0 & 0 \\ 0 & 0 & 1 & 0 \\ 0 & 0 & 0 & 1 \end{pmatrix}$$

refining the structure as pseudo-merohedrally twinned proceeded without further complications. All oxygen positions were located and in the final model found to be best described in the primary unit cell.

The compounds $[Sb_4O_{7+3\delta}X_4][Zn_3]_{1+\delta}$, (X = Cl, Br, I), $\delta \approx 0.2$ are isostructural, and may be described by the behavior of the iodide compound without loss of generality. The Br compound produced crystals of relatively low quality, and for these convergence was difficult to achieve. The problem was solved by restricting all oxygen thermal displacement parameters to be equal. The non-stoichiometry originates from the composite nature of the structures. The primary unit cell is the locus of

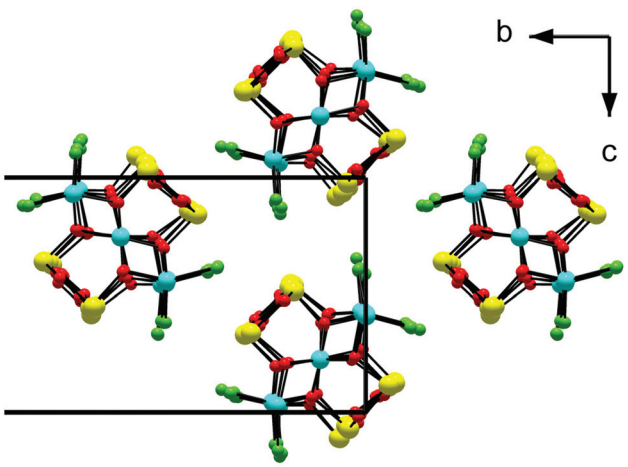

Fig. 3 Structure of single columns of $SbZn_{1-y}O_{2-y}I$ viewed along a. Zinc (blue) is coordinated entirely by oxygen (red) or by oxygen and iodine (green), whereas antimony forms oxygen-connected ladders. Note the exposure of Sb to the surroundings of the column, a typical trait of lone-pair behavior.

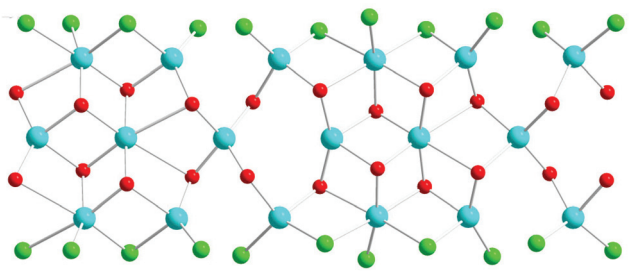

Fig. 4 *Coeur-du-filé* of a single column of the structure, displaying the misfit between on one hand Zn(blue) and on the other hand oxygen (red) and I (green). The a direction is horizontal.

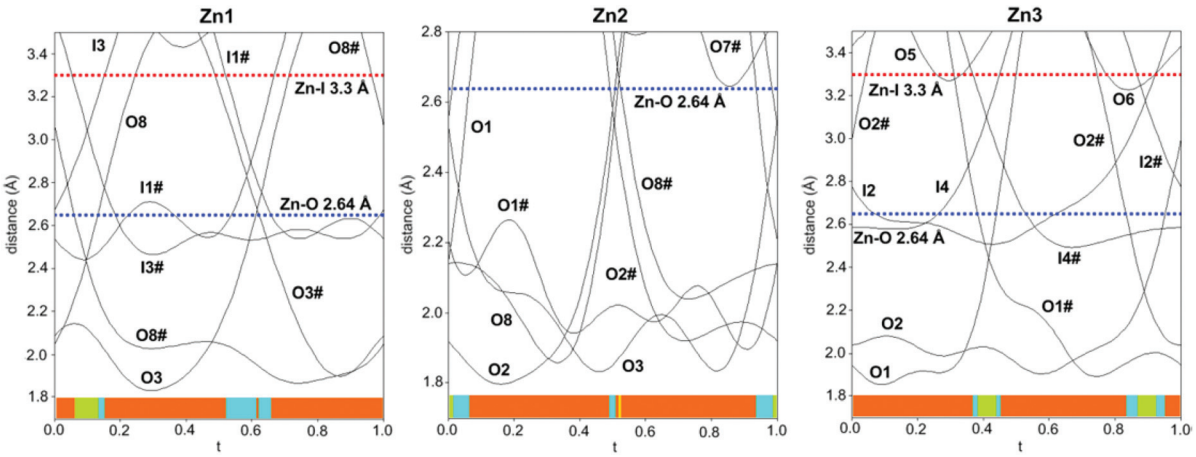

Fig. 5 Variation in the coordination around the three crystallographically different Zn-atoms in the form of *t*-plots. The maximum Zn–O and Zn–I distances to be considered for covalent bonding are indicated with dotted lines. The coordination number is outlined with colored bars; yellow = 3-coordination, red = 4-coordination, blue = 5-coordination, and green = 6-coordination. # sign implies symmetry-equivalent atoms.

the $Sb_4O_8I_4$ sub-structure, whereas the secondary unit cell given by the relationship $a_2^* = a_1^* + q$, $b_2^* = b_1^*$, $c_2^* = c_1^*$ yielding a = 3.4797 Å, b = 18.508 Å, c = 10.7768 Å, β = 97.915°, q = (α0γ), α = 0.1852, γ = 0.3451 contains Zn only. This model refines very well yielding R_1 values better than 6% for main reflections and better than 12% and 18% for first- and second-order satellites, respectively. The number of Sb positions in the primary cell is 4, whereas the number of Zn positions in the secondary cell is 3. However, because of the metric relationship between the two unit cells, the relative amount Sb : Zn is not 4 : 3, but rather 4 : 3.682; that is, because the Zn content refers to a smaller cell, it must be multiplied by the ratio of the *a*-axes of the two cells, 4.271/3.4797. This still leaves the structure unbalanced with respect to charge, for which there are several possible remedies. The answer might be found in the partial replacement of O by OH, the oxidation of Sb(III) to Sb(V) or the under-occupancy of either oxygen or iodine. The oxidation of Sb is unlikely because of the absence of oxidizing agents in the synthesis and the local coordination of Sb that clearly indicates the trivalent state throughout the structure. Similarly, the absence of iodide should be very noticeable as negative residual electron density. The most likely charge compensation is therefore either partial occupancies on oxygen and/or the presence of hydrogen in the structure. The latter can hardly constitute the sole contribution to charge balance because this would require a rather substantial moisture content in the reaction mixture. Given that the title compounds are the main product of the reaction, the required hydrogen content is $[Sb_4O_{7.38}(OH)_{0.62}I_4][Zn_3]_{1.23}$, rather more than expected from only contaminant water. This leaves oxygen vacancies as the only plausible main contributor to balance the charge of the non-stoichiometry.

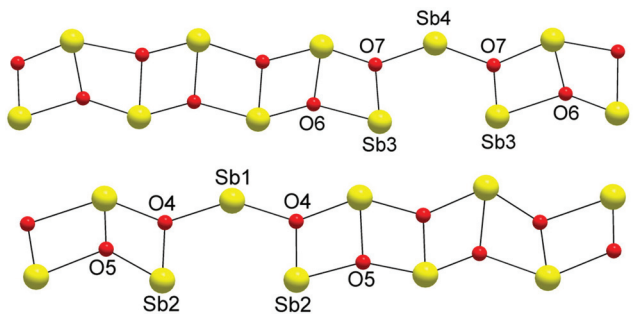

Fig. 6 Two types of Sb–O ladders. Note that oxygen vacancies balance the charge deficiency. In one ladder, there are O6 vacancies, and in the other, O5 vacancies.

It was found that bond valence sum calculations were quite a useful tool in this quest. While the BVS for all the Sb positions vary, the BVS of Sb1 stands out as singular, reaching a maximum value of well above four. A closer inspection reveals that the high value of this BVS is caused by a short Sb1–O5 distance over part of a range of the internal coordinate, describing the propagation of the structure along the direction of the ***q***-vector. Introducing occupational modulation on position O5 yields an improvement of the fit of the model to the data and reduces the offending BVS value to one more on par with those of the other Sb positions. The reduced occupancy of O5 also brings the compound closer to an overall charge balance. A somewhat less problematic but still high BVS is found for Sb3, and herein, the cause is a short distance to O6. Following the procedure for O5, an occupational modulation was introduced for O6, which led to further improvement and a change in composition to slightly below the ideal value $[Sb_4O_{7.69}X_4]$-$[Zn_3]_{1.23}$. In the final model, the sum of the occupancies for positions O5 and O6 was set at 1.69 to avoid overcompensating for Zn deficiency. Unsurprisingly, the agreement between model and data is quite insensitive to such small changes in oxygen content.

The structure is composed of columns centered by three Zn positions, with the central being coordinated exclusively by oxygen, whereas the two outer columns also bind to Cl/Br/I.

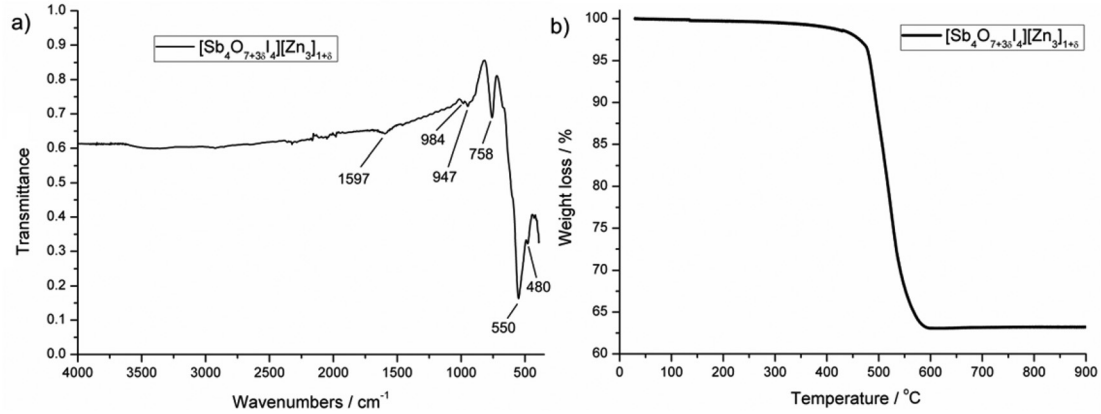

Fig. 7 (a) FT-IR spectrum and (b) TG curve of $[Sb_4O_{7+3\delta}I_4][Zn_3]_{1+\delta}$.

The oxygen atoms are further connected to Sb atoms belonging to Sb–O ladders. The structure looks rather simple when viewed along the *a* direction (see Fig. 3). In a perpendicular view, the complexity becomes more pronounced. The mismatch between Zn and the rest of the structure is most easily seen if the Sb–O ladders are removed from the column (see Fig. 4). The coordination around the three Zn atoms is clarified with *t*-plots (see Fig. 5) to show how the coordination number varies, depending on the modulation. The composite nature of the structure leads to a charge imbalance that is compensated by oxygen vacancies, which are located in one of the Sb–O ladders (see Fig. 6). The Sb–O ladders are strongly reminiscent of the ones in $Sb_8O_{11}X_2$.[5,6] The electron density maps show that the atomic modulation functions capture the behavior of each atomic position well (see ESI†).

Almost phase-pure material (see powder diffractogram in ESI†) could be synthesized for the iodine compound, which was used to collect an IR spectrum and to study thermal decomposition. Fig. 7a shows the transmission IR spectrum for $[Sb_4O_{7+3\delta}I_4][Zn_3]_{1+\delta}$ in the range 4000 to 400 cm^{-1}. Intense peaks are observed in the low-energy region, which are most probably due to Sb–O and Zn–O vibrations. The absence of peaks in the high-energy region confirms the absence of hydroxyl groups, which would give rise to strong signals. Thermogravimetry (TG) data of $[Sb_4O_{7+3\delta}I_4][Zn_3]_{1+\delta}$ were recorded from 30–900 °C in a nitrogen atmosphere with a heating rate of 5 °C min^{-1}. The TG curve in Fig. 7b shows that the compound is stable up to 400 °C and decomposes shortly thereafter in a single step by releasing iodine as I_2(g). This is in good agreement with the total weight loss of about 37%. A powder diffraction pattern of the decomposition product shows a mixture of the oxides $ZnSb_2O_6$ and $Zn_{2.33}Sb_{0.67}O_4$, which implies that antimony has been oxidized to Sb(v).

Conclusions

The new isostructural compounds $[Sb_4O_{7+3\delta}X_4][Zn_3]_{1+\delta}$, (X = Cl, Br, I), $\delta \approx 0.2$ were synthesized *via* chemical reactions in evacuated and sealed silica tubes. The crystal structure was found to be incommensurately modulated and was refined in the monoclinic 3 + 1 dimensional space group $P2_1(\alpha 0\gamma)0$ having a $\boldsymbol{q}$ vector in the *ac*-plane. The close-to-perfect orthorhombic pseudo-symmetry of the fundamental unit cell and the presence of two (orthorhombically) symmetry-equivalent $\boldsymbol{q}$-vectors results in pseudo merohedral twinning. The structure consists of one-dimensional columns having the Zn atoms in the center to which ladders of antimony oxides are attached. The domination of first-order and second-order satellites for 1*kl* and 2*kl* reflections, respectively, strongly indicate a composite behavior and that all the Zn atoms were described in a second composite unit cell. The overall charge balance was obtained by introducing oxygen vacancies in the antimony ladders, which is supported by bond valance sum calculations and by the IR measurements that do not show any signs of hydroxyl groups being present. From TG, one can observe the decomposition of the iodide phase in a single step above 400 °C by releasing I_2(g) and oxidising antimony to Sb(v).

Acknowledgements

The Swedish Research Council is acknowledged for financial support.

References

1 Z. Mayerová, M. Johnsson and S. Lidin, *J. Solid State Chem.*, 2005, **178**, 3471–3475.
2 Z. Mayerová, M. Johnsson and S. Lidin, *Angew. Chem., Int. Ed.*, 2006, **45**, 5602–5606.
3 R. Becker, M. Johnsson, R. K. Kremer and P. Lemmens, *Solid State Sci.*, 2003, **5**, 1411–1416.
4 S. Menchetti, C. Sabeli and R. Trosti-Rerroni, *Acta Crystallogr., Sect. C: Cryst. Struct. Commun.*, 1984, **40**, 1506–1510.
5 Z. Mayerová, M. Johnsson and S. Lidin, *Solid State Sci.*, 2006, **8**, 849–854.

6 S. Lidin, M. Johnsson and Z. Hugonin, *Solid State Sci.*, 2009, **11**, 1198–1205.
7 J. Sun, S. Lee and J. Lin, *Chem. – Asian J.*, 2007, **2**, 1204–1229.
8 B. D. Cutforth, *Preparation, Structural Characterization and Electrical Properties of Some Polyatomic Cations of Mercury*, Open Access Dissertations and Theses, Paper 3741, McMaster University, Canada, 1975.
9 I. D. Brown, B. D. Cutforth, C. G. Davies, R. J. Gillespie, P. R. Ireland and J. E. Vekris, *Can. J. Chem.*, 2011, **52**, 791–793.
10 M. Evain, F. Boucher, O. Gourdon, V. Petricek, M. Dusek and P. Bezdicka, *Chem. Mater.*, 1998, **10**, 3068–3076.
11 N. A. Jordan, P. D. Battle, S. van Smaalen and M. Wunschel, *Chem. Mater.*, 2003, **15**, 4262–4267.
12 M. Zakhour-Nakhl, J. B. Claridge, J. Darriet, F. Weill, H.-C. zur Loye and J. M. Perez-Mato, *J. Am. Chem. Soc.*, 2000, **122**, 1618–1623.
13 A. E. Abed, E. Gaudin, H.-C. zur Loye and J. Darriet, *Solid State Sci.*, 2003, **5**, 59–71.
14 S. Stahl, *Ark. Kemi, Mineral. Geol.*, 1943, **17**, 1–7.
15 L. Palatinus and G. Chapuis, *J. Appl. Crystallogr.*, 2007, **40**, 786–790.
16 V. Petříček, M. Dušek and L. Palatinus, JANA-2006, Institute for Physics AVCR, Praha, Czech Republic, 2006.
17 S. van Smaalen, *Phys. Rev.*, 1991, **B43**, 11330–11341.
18 S. van Smaalen, *Crystallogr. Rev.*, 1995, **4**, 79–202.
19 K. Brandenburg, *DIAMOND, Release 2.1e*, Crystal impact GbR, Bonn, Germany, 2000.